Available online at www.sciencedirect.com
SCIENCE DIRECT®
International Journal of Heat and Mass Transfer 47 (2004) 3355–3373
International Journal of HEAT and MASS TRANSFER
www.elsevier.com/locate/ijhmt

Multi-factorial study of the absorption process of H_2O(vap) by a LiBr(aq) in a horizontal tube bundle using 2-ethyl-1-hexanol as surfactant

Victor Manuel Soto Francés *, José Manuel Pinazo Ojer

Departamento de Termodinámica Aplicada, Universidad Politécnica de Valencia, Camino de Vera S/N, 46022 Valencia, Spain

Received 28 December 2002; received in revised form 22 January 2004
Available online 17 April 2004

Abstract

This paper presents the results of a series of experimental tests about the absorption of water vapour by an aqueous lithium bromide solution over a bundle of 14 smooth tubes, using an alcohol (2-ethyl-1-hexanol) as surfactant. It follows the same multi-factorial methodology used in a previous article, in order to compare with the experiences without the alcohol. The study reveals that the 2-ethyl-1-hexanol strongly affects the hydrodynamics and the heat and mass transfer as is already known. However, new insight about the absorption process is gained by comparing our experiences with less common theoretical works on falling film stability where some parallelisms are identified. As a result, the main parameters that control this dynamic process seem to be the Marangoni number and also the Reynolds number, as many authors would point out as obvious. But it is much less obvious, that they do interact with each other to create a *stability window and to determine the pattern of the flow and therefore the mass transfer rate*. Finally in the conclusions a comment on how this could be used in practice is also done and some further research proposed, as for instance, the implication, or not, of the Soret effect in the inter-phase dynamics of the surfactant (2-ethyl-1-hexanol in our case) for aqueous lithium bromide solutions.

Keywords: Absorption; Lithium bromide absorption machines; Absorber; Falling film; Additives; Marangoni effect

1. Introduction

The optimal design of absorption cooling machines [1,2] has shown that a high value of AU needs to be installed at the absorber component in order to achieve high efficiencies. A lot of research has been done to design an absorber with an U value as high as possible which allows a reduction in the amount of area A installed at the absorber section and thus makes the machine more compact and competitive with respect to the compression cooling machines. Of course, together with this increase in the heat transfer capability U, the mass transfer process should be promoted. This latter transfer process, in our opinion, is seldom treated with enough detail.

A common practice to rise the U and the mass transfer coefficient β, among other solutions, is the use of additives or surfactants (mainly in the case of LiBr–H_2O machines). Their use was firstly intended to avoid the wetting problems of the tubes (see Soto Francés and Pinazo Ojer [3]) but it was found by chance that some other effects were present.

Although Pearson [4] already in 1958 pointed out the existence of surface tension effects in drying paint films, Kashiwagi et al. [5] was one of the first to point out that the Marangoni instability (i.e. convection due to surface tension gradients) seemed to be the reason for the observed turbulence at the interface between the water vapour and the aqueous LiBr solution. He made the hypothesis that for the onset of the instability it was

* Corresponding author. Tel.: +34-6-387-9326; fax: +34-6-387-7329.
E-mail address: vsoto@ter.upv.es (V.M. Soto Francés).

0017-9310/$ - see front matter © 2004 Elsevier Ltd. All rights reserved.
doi:10.1016/j.ijheatmasstransfer.2004.01.024

Nomenclature

Re	Reynolds number, $4\Gamma/\mu$
Ma	Marangoni number
(E^2/D)	evaporation number, $(\lambda\Delta T/\rho v\Delta h_{abs})^2/(3/2\rho_{vapour}/\rho_{liquid})$
W	LiBr mass fraction (wt.%)
D	Fick's diffusivity coefficient for the LiBr ($m^2\,s^{-1}$)
P	pressure (Pa)
Δh_{abs}	enthalpy of absorption ($J\,kg^{-1}$ water) (enthalpy of the water vapour − partial enthalpy of water in the solution)
A	absorber area (m^2)
U	overall heat transfer coefficient ($J\,s^{-1}\,m^{-2}\,K^{-1}$)
Q	heat transferred to the cooling water ($J\,s^{-1}$)
F	non-dimensional heat exchanger correction factor
H	convection heat transfer coefficient ($J\,s^{-1}\,m^{-2}\,K^{-1}$)
rq	non-dimensional heat ratio
$\dot{V}$	volumetric flow rate ($m^3\,s^{-1}$)
$\dot{m}$	mass rate ($kg\,s^{-1}$)
k	wave number ($2\pi/L$), L wave length
I	instability region
S	stability region

Greek symbols

Γ	peripherical mass flow rate referred to one side of the tube ($kg\,s^{-1}\,m^{-1}$)
ρ	density ($kg\,m^{-3}$)
β	mass transfer coefficient ($m\,s^{-1}$)
μ	dynamical viscosity ($N\,s\,m^{-2}$)
v	kinetic viscosity ($m^2\,s^{-1}$)
δ	film thickness (m)
α	non-dimensional scaling factor
λ_0, λ	heat conductivity ($J\,s^{-1}\,m^{-1}\,K^{-1}$)
σ	surface tension ($N\,m^{-1}$)
Σ_s	surface of neutral stability. It separates stable and unstable regions

Superscripts

*	equilibrium
$\bar{}$	average
$'$	modified definition (applied to the Marangoni number)

Subscripts

cw	cooling water
i	inlet
o	outlet
c	critical
s	separation between a sub-critical and supercritical instability

necessary the existence of droplets of additive over the surface of the solution. Latter on, Hihara and co-workers [6,7] showed that concentrations of additive below its solubility limit were also able to produce enhancements in the transfer rates. For a more detailed historical review the reader may refer to Ziegler and Grossman [8].

Since then, many experimental and theoretical studies on stability have been conducted. At the experimental level it is easy to find works about the effect of different surfactants or even a mixture of them [9] added into a static pool of solution (i.e. $Re = 0$). However the extrapolation of these results to absorbers used in commercial machines, normally of the horizontal tube bundle type, is not so straightforward (since $Re \neq 0$). That is the reason why authors like Miller [10] or Greiter et al. [11] studied the problem in a more realistic absorber configuration, and this is also our case.

The horizontal tube absorber with a falling film of solution driven by gravity is a very common configuration in machines. This work studies the behaviour of the heat and mass transfer process, during the absorption of water vapour into a falling film of LiBr solution, over a horizontal tube bundle of smooth tubes with 2-ethyl-1-hexanol as additive. The paper is divided into four main sections:

1. *Description of the test ring and pose of the experiences.* In this section the set-up is described and the phenomenological heat and mass transfer coefficients are defined and discussed. Afterwards the multi-factorial pose of the experiences is explained. Though a section similar to this appeared also in [12], but for the device for adding the alcohol to the vapour phase, we have included it here for completeness and because we consider that the definition of the transfer coefficients deserves to be included. Mainly the mass transfer coefficient which is different from other authors.

2. *Theoretical studies about stability of falling films.* In our opinion there is a realm of unconnected information between the more pure and the more applied, scientific literature. We have tried to shrink a little this region, by including this section and Section 5. As mentioned before, studies on falling film stabilities ($Re \neq 0$) with Marangoni effects are difficult to find and to understand. This section tries to give some insight at this respect.

Here we start with a discussion about the origin of the changes of surface tension during absorption. The section follows with the falling film behaviour by a description of a linear stability map (small perturbation of the film thickness) and ends with the non-linear evolution of the film thickness for pure hydrodynamic instability and for the coupling between the hydrodynamic and the capillary instabilities.

3. *Raw processing of the experimental results.* This section shows the results of the raw processing, according to our multi-factorial scheme, of the results obtained from the experiences. Also a general comment on the behaviour of the heat and mass transfer processes is included.

4. *Relationship between the theoretical studies exposed in Section* 3 *and our experiences in Section* 4. As a consequence of what is exposed in Section 3, we need to view the experimental results in a Marangoni–Reynolds plane for comparison with the theoretical ones. However some care must be taken when building the Marangoni axis and when relating the empirical results with theory. All this is discussed under the title; ''Scaled Marangoni–*Re* plane (*Ma*′–*Re*)''. Once this plane is introduced, the discussion may follow with the comparison between the theoretical and the observed results from the experiences.

We are aware that the subject is not easy but our aim in the paper has been to show; on one hand how we obtained the experimental results and in the other how they seem to articulate with more basic theoretical research, thus gaining more insight about the absorption process. Finally, in the conclusions, we point out where more research is needed and in which way, all this work, may be used in practice.

2. Description of the test ring and pose of the experiences

2.1. Experimental set-up

Basically the experimental set-up and the absorber configuration corresponds to the one presented in a previous article [12]. The absorber tube bundle is composed of 14 smooth copper tubes of 15.9 mm of outer diameter. The axes of the tubes were separated 46.9 mm. Fig. 1 shows a scheme of the installation. The main difference with respect to the previous scheme, is the presence of a device to add the 2-ethyl-1-hexanol directly to the vapour phase. It consists of a graduated tube filled with the alcohol. One end is open to the atmosphere while the other is connected to the vapour phase of the set-up, through a diaphragm valve. When the valve is opened the atmospheric pressure pushes the alcohol into the facility. The amount of LiBr solution charged in the set-up was measured at the beginning of the essays and therefore by controlling the volume difference of alcohol added to the solution, its concentration could be inferred.

The alcohol was added to the vapour phase because some authors [10,13] have pointed that the action of the alcohol is related to its presence at the vapour phase. A discussion about this point is found in a subsequent section.

In order to follow the discussion of the results and for completeness the magnitudes measured are reproduced here:

At the absorber section:

- The water vapour pressure (capacitive sensor, P (see Fig. 1)).
- The temperature evolution of the cooling water. A differential temperature measurement was used between each pair of tubes (see Soto Francés et al. [3,14]).

At the cooling water circuit:

- The cooling water temperature, at the inlet ($T_{cw,i}$) and outlet ($T_{cw,o}$) (Pt-100) and its volumetric flow rate (rotameter M3). The electrical heater D2 and the plate heat exchanger HX1 were used to adjust $T_{cw,i}$.

At the solution distribution circuit:

- Solution temperature at the inlet (T_i) and outlet (T_o) (Pt-100), and the solution mass flow rate (electromagnetic flow meter, M2). The plate heat exchanger HX2 and electrical heater D1 were used to adjust T_i.

At the concentration measurement circuit:

- Density and temperature of the solution, at the pool and the outlet of the absorber (Coriolis mass flowmeter, M1). These two magnitudes were used to estimate the salt mass fraction (W_o).

Auxiliary devices and circuits:

- The recirculation circuit was used for recirculating the solution in order to keep the pool concentration uniform during the tests. At the begining of each test the valves of this circuit were used to measure the pool concentration (W_i) with the flowmeter M1. This circuit also had a floating densimeter D3 for checking visually the pool density.

2.2. Definition of the heat and mass transfer phenomenological coefficients

Generally, in mass transfer problems, determination of the interfacial concentration is very important. However, in absorption plants is very difficult to measure that concentration and for that reason it is very common that researchers define an average mass transfer coefficient using more accessible data. These data is taken normally at the inlet and outlet of the absorber for the lithium bromide solution.

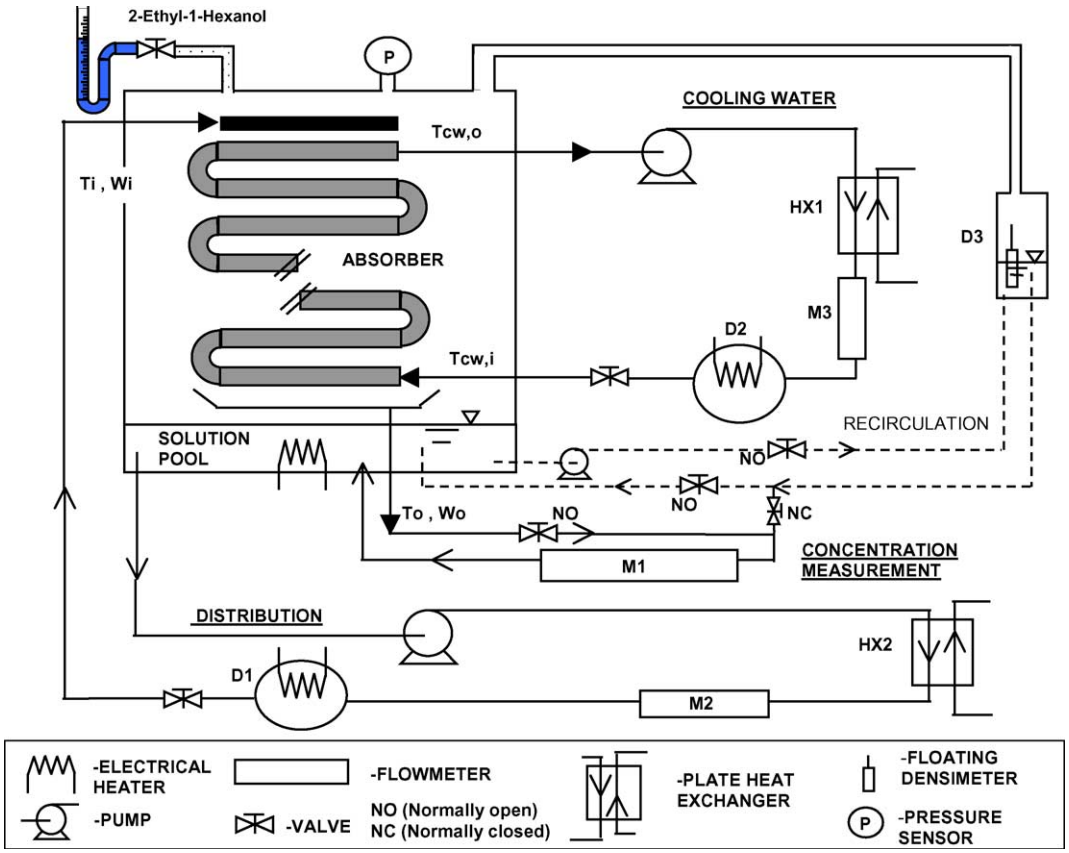

Fig. 1. Scheme of the set-up. Note the detail of the device for adding 2-ethyl-1-hexanol directly to the vapour phase. The three main circuits are shown: the cooling water circuit, the concentration measurement and the distribution of solution over the horizontal tube bundle.

Therefore for the average mass transfer coefficient (β), we used the following definition:

$$\beta = \frac{\dot{m}_{\text{absorbed}}}{A\rho\Delta W},$$

$$\Delta W = \frac{(W_{\text{i}} - W^*(P, T_{\text{cw,o}})) - (W_{\text{o}} - W^*(P, T_{\text{cw,i}}))}{\ln\left(\frac{(W_{\text{i}} - W^*(P, T_{\text{cw,o}}))}{(W_{\text{o}} - W^*(P, T_{\text{cw,i}}))}\right)} \quad (1)$$

This definition is preferable to other used for example by, Lars [15] or Miller [10] (see Eq. (2)).

$$\beta = \frac{\dot{m}_{\text{absorbed}}}{A\rho\Delta W},$$

$$\Delta W = \frac{(W_{\text{i}} - W^*(P, \overline{T}_{\text{i}})) - (W_{\text{o}} - W^*(P, \overline{T}_{\text{o}}))}{\ln\left(\frac{(W_{\text{i}} - W^*(P, \overline{T}_{\text{i}}))}{(W_{\text{o}} - W^*(P, \overline{T}_{\text{o}}))}\right)} \quad (2)$$

The main difference between Eqs. (1) and (2), is that the equilibrium concentration W^* is calculated in the former using the cooling water temperature, while in Eq. (2) the mean temperature of the solution is employed. The reason for this change is that in case the mass transfer rate is high enough, such that the heat transferred from the falling film to the cooling water is lower than the heat released by the absorption of the vapour, it is possible for the mean temperature of the solution at the outlet $\overline{T}_{\text{o}}$ to increase, although the solution remains still sub-cooled. This increase could lead, and in fact does with 2-ethyl-1-hexanol, when used in Eq. (2) together with the actual vapour pressure P, to an equilibrium salt concentration at the outlet ($W^*(P, \overline{T}_{\text{o}})$) greater than its actual value (W_{o}) at the outlet and therefore the logarithm would have a negative argument in Eq. (2). In short, although the mass transfer is an internal process, its practical driving force should be coupled in fact to the external conditions as Eq. (1) does. Moreover, this equation is always well defined since at each section of the absorber the lowest possible temperature of the falling film is the temperature of the cooling water at that section and therefore the lowest possible concentration of salt for the solution at that point is given by the equilibrium relationship ($W^*(P, T_{\text{cw}})$).

The mass absorbed m_{absorbed} was estimated using the measured solution density ρ_{i} and the value of the volumetric flow rate of solution V_{i} at the distributor inlet,

together with the change in the salt concentration between the inlet and outlet:

$$\dot{m}_{\text{absorbed}} = \dot{m}_{\text{i}}\left(\frac{w_{\text{i}}}{w_{\text{o}}} - 1\right) = \rho_{\text{i}}\dot{V}_{\text{i}}\left(\frac{w_{\text{i}}}{w_{\text{o}}} - 1\right) \tag{3}$$

When looking at the measured values of β, it is necessary to have in mind that in the present case where alcohol has been added, the ongoing transfer process takes place in a ternary system (alcohol + LiBr + H_2O). However since the alcohol is very diluted, Eq. (1) has been retained to define a single mass transfer coefficient β. This allows the comparison with the previous results. Moreover, according to [12] the Soret effect is likely to be present for the case without additive and as the concentration of alcohol is small, some of the Soret effect might be present here as well and this would force the addition of a "driving potential" affecting the mass transfer, due to the temperature gradient. This reasons turn the problem much more complex.

For the heat transfer the following expressions were used:

$$Q = AUF\,\Delta \ln T \tag{4}$$

$$\Delta \ln T = \frac{(T_{\text{i}} - T_{\text{cw,o}}) - (T_{\text{o}} - T_{\text{cw,i}})}{\ln\left(\frac{(T_{\text{i}} - T_{\text{cw,o}})}{(T_{\text{o}} - T_{\text{cw,i}})}\right)} \tag{5}$$

The absorber is treated as a counter-current heat exchanger. The corrective factor F is very close to unity (see Lars [15]). After measuring experimentally U, the film heat transfer coefficient h_{film} is obtained from Eq. (6) where the h_{cw} was determined experimentally by the same procedure as in [12] giving a value of 4039 $\text{W m}^{-2}\,^{\circ}\text{C}^{-1}$.

$$\frac{1}{U} = \frac{r_{\text{e}}}{h_{\text{cw}} r_{\text{i}}} + \frac{r_{\text{e}} \ln\left(\frac{r_{\text{e}}}{r_{\text{i}}}\right)}{\lambda_{\text{copper}}} + \frac{1}{h_{\text{film}}} \tag{6}$$

2.3. Heat ratio parameter (rq)

Besides the β and the U–h_{film}, mass and heat transfer coefficients respectively, another parameter has been used in the study.

Many authors, as for example Miller [10], use the degree of sub-cooling as an indicator for the transfer process. However we have found that it is not a very clarifying one since it depends on the inlet solution conditions.

In order to unify the heat and mass transfer processes, into a more meaningful parameter, a heat ratio named rq was defined using the enthalpy of absorption $\Delta h_{\text{absoprtion}}$ as:

$$rq = \frac{Q}{\dot{m}_{\text{absorbed}}\,\Delta h_{\text{absorption}}} \tag{7}$$

Roughly speaking, values of this heat ratio above 1 mean that the sensible cooling of the film exceeds the latent heat transferred by absorption. As it will be shown in Sections 4 and 5 this is possible for example when the mass transfer resistance is high due to non-condensing gases or due to the accumulation of additive over the liquid–vapour inter-phase. In this case most of the heat removed from the falling film Q corresponds to its sensible cooling but no to heat released by absorbed water.

2.4. Multi-factorial test

Two levels have been chosen for each factor in the tests. Each level named as (L—low or H—high). The six factors and their ranges are shown in Table 1. This gives for the total number of combinations a value $2^6 = 64$ plus an extra central point. The central point has all the factors at a level in the middle of each range. Table 2 shows the number assigned to a run and its combination of factors. The table only shows 33 runs because the rest (those with no additive, factor F—low) are those presented in [12] but for the central point (run number 9) since now this point must contain one half the high concentration of additive. Runs with the same number here and in that previous article differ only by the presence or not of additive.

The experimental heat transfer coefficient of the film h_{film} and the mass transfer coefficient β, have been correlated to a polynomial (named response surface) whose coefficients are shown in the appendix. The resulting correlation explains the 73% for the dependency of both parameters on the factors.

Based on these polynomials, the direct influence of each factor on the transfer coefficients obtained from the

Table 1
Name of the factors used in the multi-factorial and their levels

Name of the parameter	Levels
(A) w: Concentration of the LiBr salt at the inlet = pool concentration	50–60 wt.%
(B) T_{i}: Solution temperature at the inlet	303.15 K (30 °C)–308.15 K (35 °C)
(C) T_{pool}: Temperature of the pool	313.15 K (40 °C)–319.15 K (46 °C)
(D) Γ: Peripherical mass flow rate	0.01–0.045 $\text{kg m}^{-1}\,\text{s}^{-1}$
(E) m_{c}: Mass flow rate of cooling water	0.044–0.0667 kg s^{-1}
(F) Additive (2-ethyl-1-hexanol)	0–333 M ppm

Table 2
Number assigned to each run

Run	W (wt.% salt)—solution—(A)		T_{cwi} (°C)—cooling water—(B)		T_{pool} (°C)—solution—(C)		Γ ($kg\,m^{-1}\,s^{-1}$)—solution—(D)		V_{cw} ($l\,s^{-1}$)—cooling water—(E)		Measured (2E1H)	
											$\beta \times 10^5$ ($m\,s^{-1}$)	h_{film} ($W\,m^{-2}\,K^{-1}$)
1	L	53.28	H	35.68	L	41.21	L	0.0160	L	0.044	1.213	488
2	H	61.65	L	30.08	H	46.39	L	0.0186	L	0.044	1.149	457
3	L	53.13	L	30.83	H	46.36	H	0.0416	H	0.067	4.718	1562
4	H	61.65	H	35.64	H	46.36	L	0.0126	L	0.044	0.479	479
5	L	55.75	L	30.41	L	40.22	H	0.0469	H	0.067	3.270	1023
6	H	61.65	H	34.66	H	46.32	H	0.0492	H	0.067	1.885	908
7	H	61.65	H	35.64	L	40.17	H	0.0489	L	0.044	0.435	778
8	H	61.65	H	35.26	L	41.15	L	0.0160	H	0.067	0.148	322
9	LH/2	54.87	LH/2	33.13	LH/2	43.25	LH/2	0.0197	LH/2	0.055	0.230	780
10	L	52.70	L	27.44	H	46.3	H	0.0463	L	0.044	2.654	986
11	L	52.70	L	30.52	H	46.31	L	0.0118	H	0.067	1.572	939
12	H	61.46	L	30.52	H	46.29	H	0.0525	H	0.067	2.106	1037
13	L	52.70	L	30.28	H	46.31	L	0.0136	L	0.044	1.489	936
14	H	60.80	L	30.67	H	46.43	L	0.0168	H	0.067	0.276	391
15	H	61.08	L	30.60	L	41.29	H	0.0503	H	0.067	0.323	1127
16	L	53.13	L	30.94	L	41.39	L	0.0132	H	0.067	0.872	510
17	L	53.28	H	35.39	L	41.22	H	0.0427	H	0.067	2.374	889
18	L	52.70	H	35.99	H	46.31	L	0.0150	L	0.044	1.708	741
19	H	61.08	L	29.97	L	41.21	L	0.0141	L	0.044	0.143	427
20	L	53.13	L	30.47	L	41.41	H	0.0485	L	0.044	2.321	1178
21	H	61.65	H	35.35	L	40.21	H	0.0486	H	0.067	0.458	633
22	H	61.65	H	30.42	L	41.31	H	0.0136	H	0.067	0.147	324
23	L	53.13	L	30.53	L	41.41	L	0.0126	L	0.044	0.745	675
24	H	61.08	L	29.97	L	41.21	H	0.0494	L	0.044	0.257	1181
25	H	60.80	H	36.35	H	46.3	L	0.0141	H	0.067	0.192	325
26	L	52.70	H	34.79	H	46.28	H	0.0490	H	0.067	3.641	1375
27	H	61.65	L	30.30	H	46.41	H	0.0449	L	0.044	2.183	1281
28	L	53.13	H	35.79	H	46.40	L	0.0122	H	0.067	2.214	824
29	L	52.70	H	35.95	H	46.33	H	0.0470	L	0.044	3.460	1831
30	L	53.13	H	35.94	L	41.90	L	0.0137	H	0.067	1.612	435
31	H	61.65	H	35.73	L	41.23	L	0.0152	L	0.044	0.114	275
32	L	53.28	H	35.64	L	41.22	H	0.0423	L	0.044	2.591	889
33	H	61.65	H	35.71	H	46.37	H	0.0502	L	0.044	1.077	891

Average value obtained for the film heat and the mass transfer coefficients.

experiences, together with their pair-wise interaction, can be analysed by the Pareto's Charts [14,16].

The presence of the additive, as will be described, produces a instability which makes the numerical resolution of the problem quite complex. Therefore, now the Standardized Pareto's Charts have been used to detect the influence of each experimental factor directly on the measured values (Eqs. (1) and (6)).

The x-axis is non-dimensional. It represents the standardized effect or in other words, the magnitude of the effect (change in the response) divided by its standard deviation, for a certain factor. Statistically those factors whose bars are to the right of the vertical line must be considered the most important. The charts for the effect on the h_{film} and β, due to the chosen factors (see Table 1), are shown in Fig. 2.

The response surface coefficients for the two effects are collected in the appendix.

Before going into the study of the results of the tests it is worthwhile making a short review about the film instabilities which are known as Marangoni effect. The subject is quite complex and we have tried to give the basic hints.

3. Theoretical studies about stability of falling films ($Re \neq 0$)

3.1. Who controls the changes of surface tension during absorption?

Changes in surface tension may be produced, among others, by variations in composition (LiBr salt concentration) or/and inter-phase temperature. This property may lead to film solutal-capillary or thermal-capillary instabilities, and to what is also known as interfacial

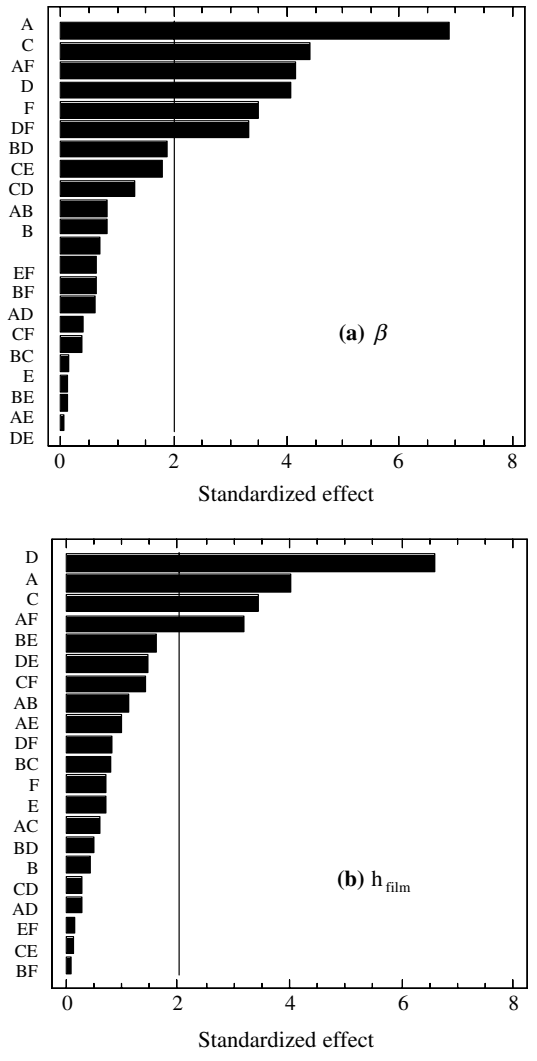

Fig. 2. Pareto's Charts which indicate the most influent factors and their binary interaction on the response magnitude. Those whose black bar crosses to the right of the vertical line are the most important. Influence on: (a) mass transfer coefficient, (b) film heat transfer coefficient.

turbulence which promotes the mass transfer. Fujita and Hihara [17], showed that for these to occur the solutal or the thermal Marangoni numbers need to be negative and positive respectively. They both compete with each other for inducing the instability (see Eq. (8)). Notice that a positive Ma_T or negative Ma_W, number means that the surface tension raises with the temperature or decreases with salt concentration respectively. He proposed two new modes of fluctuation of the inter-phase temperature, salt concentration and surface tension; one called temperature dominant and the other concentration dominant.

Assuming near equilibrium conditions at the interphase, the fluctuations can be combined into a single total Marangoni number as:

$$Ma = Ma_T + Ma_W = \left(\frac{\partial\sigma}{\partial T}\right)\frac{\delta\Delta T}{\mu\nu} + \left(\frac{\partial\sigma}{\partial W}\right)\frac{\delta\Delta W}{\mu\nu} \qquad (8)$$

3.1.1. Thermal Marangoni as dominating factor

On one hand, Fujita and Hihara [17] showed experimentally, in an static pool of solution plus additive (*n*-octanol), that the instability of Marangoni for aqueous solution of LiBr is dominated by the temperature effect, i.e., by the thermal Marangoni number and therefore $Ma_T \cong Ma > 0$. According to this mode, at the interphase, a rise in temperature must be accompanied by a rise in salt concentration (to maintain constant the vapour pressure) and a rise in surface tension (to produce the instability). Note that if the temperature rises is because water vapour has been absorbed and therefore salt concentration has been reduced. How this two trends could be reconciled, will be discussed in the next sections.

Once checked that the changes of temperature control de surface tension gradients we can proceed with the study of theoretical models which are based on this hypothesis.

3.2. Linear study: the linear stability map

On the other hand, and closer to the actual conditions of film absorption, Joo et al. [18] made a theoretical study of stability for two-dimensional films, flowing down a heated plate. They showed that for a volatile fluid when the thermal Marangoni effect is considered, a stability map can be drawn (reproduced in Fig. 3), valid for each wave number k of the perturbation—i.e. a small spatial sinusoidal variation of the film thickness—imposed to the equilibrium film thickness, also known as the base state of the film. This map has as axes; (Ma) the Marangoni number, the (Re) Reynolds number, (E^2/D) the evaporation number.

The evaporation number takes into account the destabilising effect of the vapour recoil. We have included it for completeness, nevertheless for the case of LiBr(aq), this number is much smaller than the other two and here will be disregarded.

Therefore the points which are reachable by the LiBr solution are placed on the *Ma–Re* plane. The graphs (B) and (C) of Fig. 3 show the unstable and stable *Ma–Re* regions for each imposed wave number k, which now is represented in the z-axis instead of E^2/D.

Although these plots are valid for a film flowing down a plate, it is supposed that they are at least qualitatively valid also for round tubes because the thickness of the film is small compared to the radius of the tube (in our case this ratio is around 0.01).

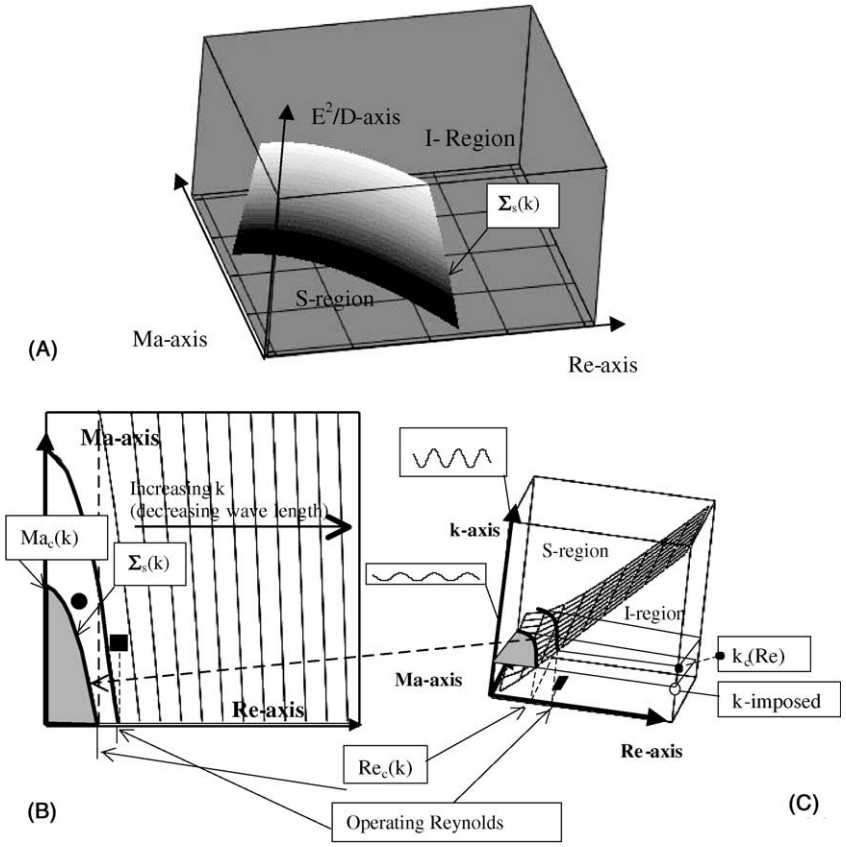

Fig. 3. Stability maps obtained from theoretical studies on falling film down a plane. Stable (*S*-region) and unstable (*I*-region) zones for a certain wave length of the imposed perturbation to the film thickness. (A) General map E^2/D—evaporation number, *Re*—Reynolds number, *Ma*—Marangoni number. If E^2/D is negligible the (C) can be drawn by using *z*-axis for the wave number k of the imposed perturbation to the film. (B) is the projection of the (C) map onto the *Re–Ma* plane.

The linear stability analysis shows that points inside the *S*-region, separated by the surface Σ_s, are stable while all points outside, in the *I*-region, are unstable. The greater their distance from Σ_s the more linearly unstable they become.

In literature the presence of this *S*-stable region leads to what is called a *stability window*. For a certain imposed wave number perturbation k, there is a critical Reynolds number $Re_c(k)$. The flow is hydro-dynamically unstable for operating Reynolds *Re* greater than this Re_c.

The position and size of this *S*-region is not fixed. High values of the mean surface tension, the hydrostatic pressure and the wave number have stabilising effects and therefore increase its size. For wave numbers above a critical value k_c (short wave lengths) the film is always stable. In other words; the longer the perturbating waves the stronger the instability.

Moreover it has to be taken into account that when additive is present besides making the sign of *Ma* positive and thus allowing the instability to occur when cooling, a certain resistance should develop at the inter-phase to the absorption of water vapour. A small quantity of additive would produce a small mass transfer resistance but also a weaker instability. At the other end, an excessive amount of additive will hinder absorption by increasing the mass transfer resistance but also a stronger instability. Therefore there should be an optimum amount of additive, related with the dynamics at the surface, that produces strong enough surface tension gradients over the inter-phase (in other words a high enough Marangoni number). Unfortunately the literature gives a no clear value due to the very difficult measurement problems during absorption.

3.3. Non-linear stability analysis

Besides the linear stability analysis, the non-linear evolution of the film starting at the obtained points of linear instability were also investigated by Joo et al. [18] and some interesting conclusions resulted about the film behaviour. A discussion about this evolution from the

point of view of chaos mechanics (turbulence) can be found as well in [19].

The starting point of Joo was the interaction between the pure hydrodynamic instability ($Ma = 0$) and the capillary effects in a 2D film using long-wave theory approximation.

3.3.1. Hydrodynamic instability

In pure hydrodynamic instabilities (without capillary effects) there is a wave number k_s (that depends on k_c) which splits the unstable region into two zones; one super-critical $k_s < k < k_c$ and another sub-critical $0 < k < k_s$. In the super-critical zone the growth of the amplitude of the fundamental disturbance is transferred to a few higher harmonics. But this secondary-flow is equilibrated or saturated by the non-linear behaviour of the flow.

If k is close to k_c a periodical almost sinusoidal wave appears since the amplitude of the low order harmonics is small, while as k gets closer to k_s these harmonics are increasingly excited and a single wave develops, as Kapitza and Kapitza [20] observed. However if $k < k_s$ the harmonics of the fundamental perturbation wave are strongly excited by the non-linear behaviour and energy is transferred to them with no equilibration.

Joo and Davis [21] also studied the 3D behaviour of such pure hydrodynamic instabilities. They found that for perturbations in the stream-wise direction the span-wise direction is always unstable and its growth is slow and grows with the *Re* number.

3.3.2. Coupling hydrodynamic and capillary instabilities

A study of the coupling between the two instabilities in 3D is found in Joo et al. [22]. The mean flow in the stream-wise direction avoids the thinning of the film while in the span-wise direction, since no mean flow exists, the thinning produced by thermo-capillarity is very effective. The interaction between the flow in both directions makes the stream-wise waves transform into span-wise waves or longitudinal waves.

Points in the *I*-region but close to Σ_s and $Re < Re_c$, are thermo-capillarly but not hydro-dynamically unstable (see the black circle of graph (B) in Fig. 3). The capillary instability makes the fundamental disturbance amplitude grow with time. However quickly after the instability is initiated the non-linear evolution makes this wave lose its energy and saturation is reached. Therefore a few low order harmonics of the film thickness generate a single wave in the stream-wise direction. However due to the 3D interaction of the flow explained before, this two-dimensional wave is prone to transform. Patterns similar to the theoretical ones presented in [22], showing longitudinal waves, have been observed during our the experiences. See Fig. 4B. The film develops into a kind of ropes or rivulets over the tubes which were wriggling slowly. Similar ones also appear in Miller [10]. This patter is also likely to appear even if $Re > Re_c$ (k-imposed) (that is if the flow is hydro-dynamically unstable) but the k-imposed $> k_s$ (the flow is in the super-critical zone). That is points close to Σ_s.

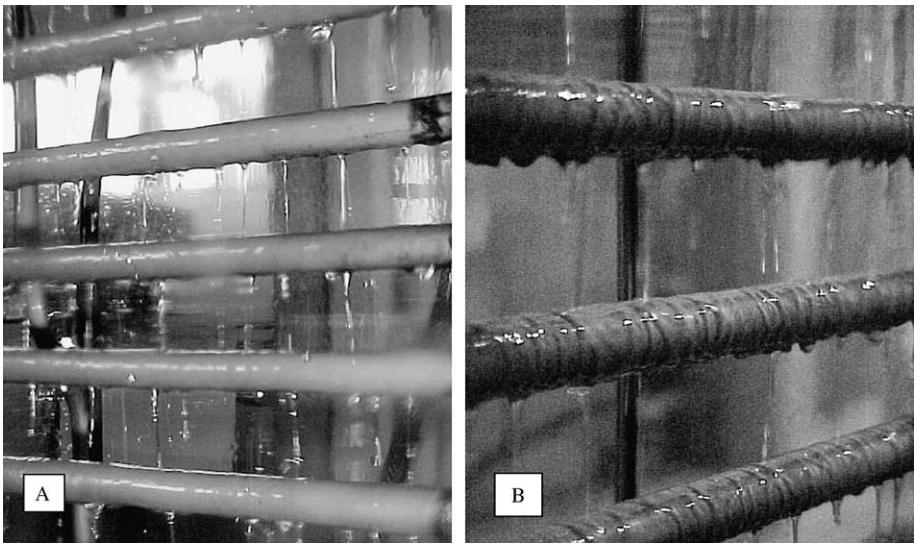

Fig. 4. Falling film pattern for the case with additive. (A) $\Gamma^+ = 0.04$, $Re = 26$, no rivulets very quiet film. The absorption process must be hindered by the additive at the inter-phase because the film is in the *S*-region. (B) $\Gamma^+ = 0.04$, $Re = 56$, moving rivulets the film is in the *I*-region but close to the Σ_s surface. *Note:* The non-dimensional peripherical mass flow rate is calculated as $\Gamma^+ = (9g/125\rho\mu\sigma^3)^{1/5}\Gamma$.

Nevertheless points far away from Σ_s, $Re > Re_c$ (see the black square of graph (B) in Fig. 3), are both thermo-capillarly and hydro-dynamically unstable. For a wave number k-imposed in the sub-critical unstable region (when considering only the hydrodynamic instability) the study shows that the coupling of instabilities produces no non-linear saturation and therefore probably a chaotic or turbulent flow. In contrast to the case of pure hydro-dynamical instability, as the perturbation wave number k increases or the Reynolds number decreases and the operating conditions move towards the stability window (super-critical conditions from the hydrodynamic point of view), the secondary-flow is never equilibrated by non-linear saturation because of the thermo-capillarity instability. Therefore in any case the film flow seems to tend to a fully chaotic or turbulent state. During our experiences, in some of the working points of the absorber—those with the higher absorption rates—the visual observation of the film, showed a very "vibrating" (at a very small spatial scale) and slightly wavy surface with no pattern (neither rivulets nor ropes as in the preceding case). These runs correspond to low salt concentrations (around 52%) and high Γ.

Therefore our visual observations of the hydrodynamics agree with this theoretical studies.

Finally, we would like to remark that although this discussion is based on theoretical studies made for a film falling down driven by gravity on a heated plate, a similar qualitative behaviour for round tubes is to be expected. It has been shown that there is already certain parallelism. Next Section 5, tries to deepen into the relationship between these theoretical studies and our tests.

4. Raw processing of the experimental results

4.1. Analysis of the multi-factorial test

Looking at the Pareto's Chart of Fig. 2, in the case of the mass transfer, the results obtained are by order of importance, according with the nomenclature of Table 1; /A/,/C/,/AF/,/D/,/F/,/DF/. While in the case of heat transfer the classification obtained are; /D/,/A/,/C/,/AF/.

Notice that both processes have the same sequence /A/,/C/,/AF/, although for the heat transfer the peripherical mass flow rate Γ (/D/ parameter), goes to the first place.

The first two parameters /A/ (salt concentration) and /C/ (temperature of the pool) strongly influence the value of the transfer coefficients by themselves, regardless of the value of the other parameters. Notice that the influence of these factors has not changed with respect to the case without alcohol (see [12]).

In the case of the concentration-additive binary interaction /AF/, Fig. 5 obtained from the adjusted response surface, shows that regardless of the value of any other factor, if the salt concentration is high (around 60 wt.%) the mass transfer is worse, while if additive is present and the concentration lower (around 50 wt.%) the trend is just the opposite. The same tendency but more stressed stands for the heat transfer coefficient of the film.

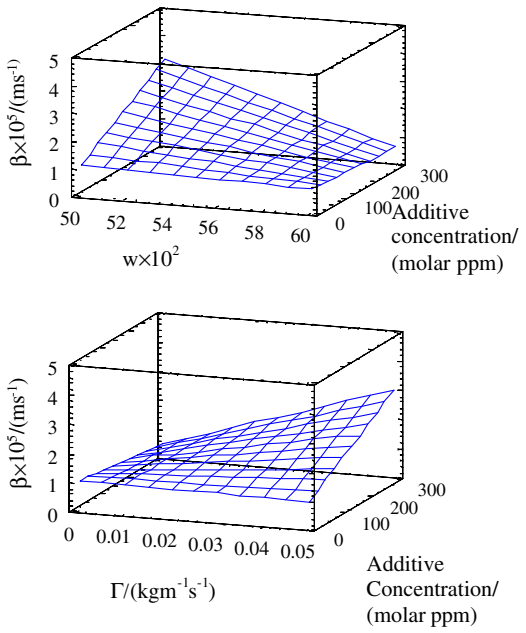

Fig. 5. Examples of the response surface of the mass transfer coefficient β. Dependence on the pair of factors: alcohol concentration/solution concentration and peripherical mass flow rate/alcohol concentration.

Finally it is worthwhile mentioning that the mass transfer process has another interesting interaction (/DF/) between the peripherical mass flow rate Γ and the additive concentration, not present in the heat transfer. As Fig. 5 shows, the flow rate and the presence of the additive seem to reinforce each other and promote the mass transfer.

4.2. General experimental results on heat and mass transfer

In this section our aim is to discuss the general trends about the transfer processes, therefore in what follows the results for each working condition are exposed gathered into two groups; one group without and the other with additive named NA and A respectively.

The estimation of the mean relative error for h_{film} has been 22%. Fig. 6 shows that the presence of the additive has a slight effect on the film heat transfer coefficient h_{film}.

Table 3 shows the average heat transfer coefficient for the NA and A groups, taking into account if the Re is

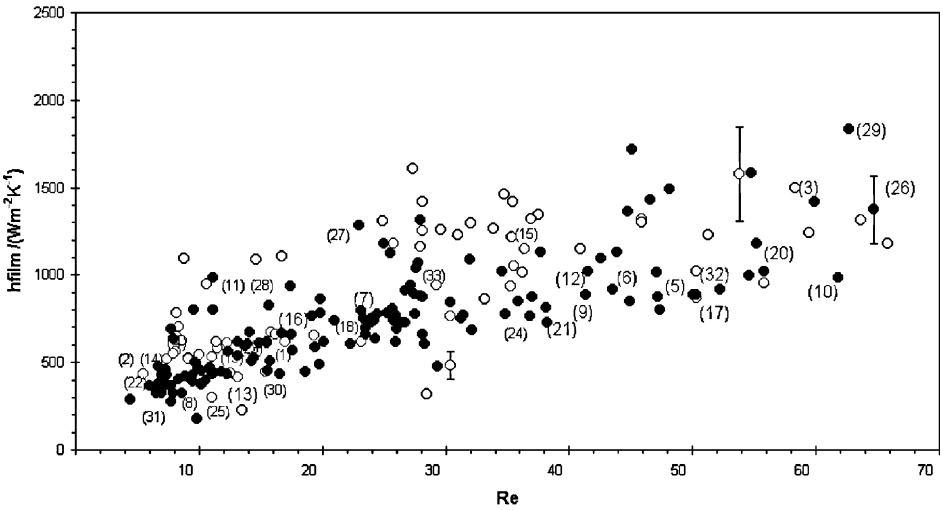

Fig. 6. Measured film heat transfer coefficient h_{film} as a function of the Reynolds number. The results are grouped into points with additive (●) and points without additive (○). Notice that this coefficient is altered but very slightly.

Table 3
Average value of the measured values of the film heat and mass transfer coefficients above and below $Re = 40$ regardless of any other parameter

Mean values	h_{film} ($W m^{-2} °C^{-1}$)		$b \times 10^5$ ($m s^{-1}$)	
	Without additive	With additive	Without additive	With additive
$Re < 40$	908	663	0.943	0.755
$Re > 40$	1221	1265	1.039	3.108

below or above 40. For *Re* below 40, the additive slightly decreases the h_{film} and the contrary occurs for the second.

Perhaps the *rq* parameter is more clarifying. Its estimated relative error is 14%. Fig. 7 shows that there is a big difference in the behaviour of this parameter with the Reynolds number for the two groups of points (NA and A). For $Re > 40$ all the points with additive have an *rq*-value below unity while the points NA are increasingly far above $rq = 1$. Note, however that for $Re < 40$ the tendency for the two groups of points is reversed.

In our opinion this means that when no additive is present the higher the *Re* number the greater the film thickness and therefore the higher the resistance to mass transfer since the temperature gradient at the inter-phase is reduced, therefore leading to a dominant sensible cooling of the film.

Finally, the estimated mean relative error for the mass transfer coefficient β was 21.6%. Fig. 8 shows also a change in the β dependency on the *Re*. For $Re > 40$ the points in the A-group (black circles) increase the mass transfer while the NA-group (white circles) has decreasing values that fall even below their values for $Re < 40$.

These results and those from the multi-factorial analysis suggest that the Reynolds number and, due to the dispersion of the values, probably another non-dimensional number/s, is playing a definite role in the transfer process. Therefore the next section includes a study about the Marangoni number.

5. Relationship between the theoretical studies exposed in Section 3 and our experiences in Section 4

5.1. Scaled Marangoni–Re plane (Ma′–Re)

In order to see if the theoretical behaviour previously described in Section 3, might match the experimental results of the multi-factorial test, the parameter *rq* and the mass transfer coefficient β have been used.

A high value of β (or a low value of *rq*) are supposed to correlate with a surface instability (mass transfer promotion). Therefore we need to represent in the *Ma*–*Re* plane the values obtained from each run of the multi-factorial test. However there is a great uncertainty in the literature about the value of the derivative $\partial\sigma/\partial T$ and the non-equilibrium state of the surface, because of

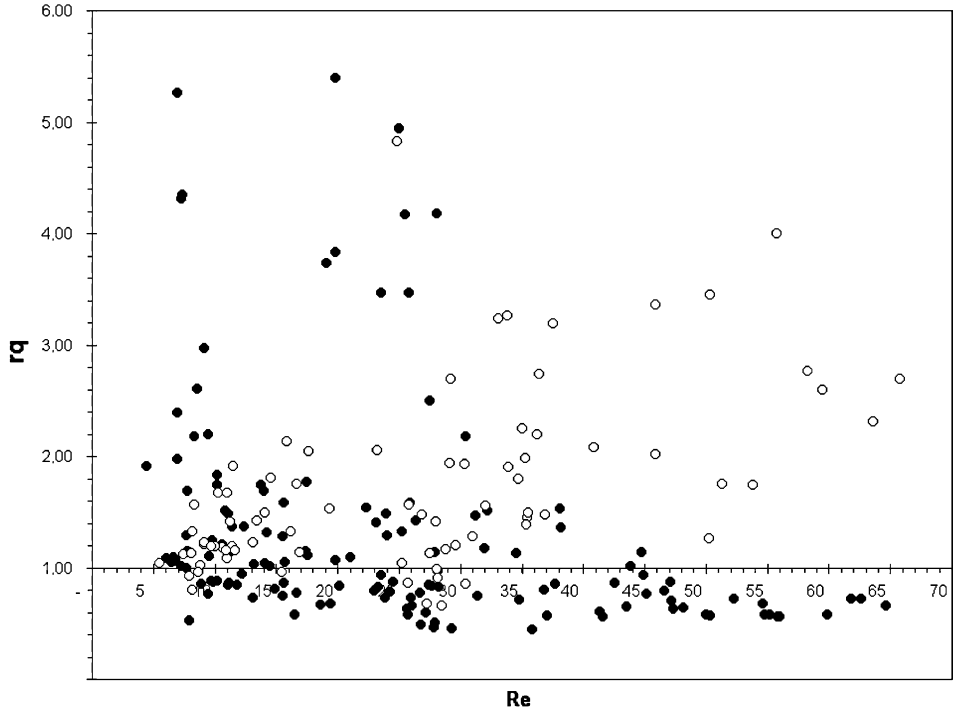

Fig. 7. Measured heat ratio *rq* parameter. High values means high sensible cooling (low absorption) with respect to absorption heat release. (●) Points with additive: notice that for $Re < 40$ the results are much more worse (high *rq*) than the case without additives what implies that the absorption is hindered. For $Re > 40$ the tendency reverses dramatically. (○) Points without additive: the sensible cooling increases monotonically with *Re* due to the increase in film thickness.

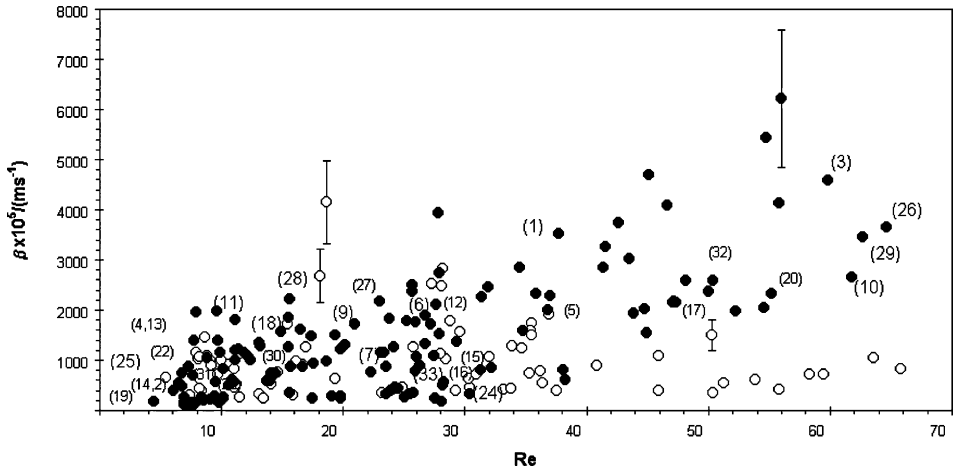

Fig. 8. Measured mass transfer coefficient β as a function of the Reynolds number. (●) Points with additive for $Re > 40$ the β are higher than for the (○) points without additive which show a maximum at $Re = 30$ and for higher *Re* the β decreases.

surface relaxation phenomena and other superficial phenomena (see Kren et al. [23]). Therefore in this paper directly a scaled Marangoni Ma' number has been used.

Based on the literature (see Daiguji et al. [6]), it has been assumed the following order of magnitude for the derivatives:

$$\left(\frac{\partial\sigma}{\partial T}\right),\left(\frac{\partial\sigma}{\partial W}\right)\approx \mathrm{O}(-4) \tag{9}$$

Since the difference ΔT is of order O(1) while Δw is of order O(−2) and according to Fujita experiments the *Ma* number is dominated by thermal Marangoni, we can make use of the Nusselt's expression for the film thickness:

$$\delta=\left[\frac{3\nu\Gamma}{\rho g}\right]^{1/3} \tag{10}$$

in order to write finally for the Marangoni number:

$$Ma\approx Ma_{\mathrm{T}}=\left(\frac{3}{4g}\right)^{1/3}(\partial\sigma/\partial T)\left[\frac{\rho Re}{\mu^4}\right]^{1/3}\Delta T \tag{11}$$

This expression shows that although *Ma* and *Re* may be fixed independently, in practice if *Re* is modified, by changing Γ for instance, then *Ma* is altered unless the ΔT is also changed. Notice also that the *Ma* number is very sensitive to the value of the viscosity and therefore to the temperature and concentration of the LiBr solution within the absorber.

The scaled Marangoni number is expressed as:

$$Ma\cdot\alpha=Ma' \tag{12}$$

$$\alpha=\frac{10^{-4}}{(\partial\sigma/\partial T)} \tag{13}$$

If the α parameter has a small variability and the order of magnitude of the derivative is close to the actual physical value, any plot using this scaled Ma' number would look like the actual plot but scaled in the *Ma* axis.

Notice also that, from the theory, for the instability to happen the derivative $\partial\sigma/\partial T$ must be positive (at least during the absorption process). Usual fluids have a negative value for it and this is also the case for the LiBr(aq). Hence the effect of the additive must be the rising of the surface tension with an increase of the interfacial temperature. From the conclusions of [12] we suspect that the Soret effect (also known as thermal diffusion) could have something to do at this respect. Keeping in mind the complexity of the problem, we suggest that perhaps a view could be the following; when water vapour is absorber onto the surface the temperature raises due to the released heat. Besides due to our hypothesis of the negative Soret effect, the ions of the salt move to the surface and hence the salt concentration increases (this would be in agreement with Fujita thermal mode). As the temperature fluctuations dominate over the concentration ones, the solubility of the alcohol would raise, thus moving itself from the liquid–vapour inter-phase into the liquid film bulk, leading to a local increase in the surface tension. However more possibilities exist that cannot be disregarded; the movement of the alcohol on the inter-phase away from the absorption location into the vapour phase, due to changes in the Van der Waals interaction with the OH– group of the alcohol (see Bennett [24]) or the diffusion of the alcohol along the surface. On the contrary, when the inter-phase decreases its temperature, the solubility of the alcohol decreases, thus decreasing the surface tension. The alcohol would go from the bulk to the surface (probably by a de-sorption controlled mechanism according to Kren et al. [23]). But its movement through the vapour phase [25], or from another place over the inter-phase by superficial diffusion is also possible. Although not definitive, Colombani in [26] says that for LiCl the negative Soret seems to be related with a change in the water polarisation away from the salt ions. This change could be affecting the adsorption of the alcohol at the inter-phase.

The visual observation supports this dynamical view of the alcohol behaviour since during the runs, where the film looked quiet (very low absorption rate, high sensible cooling), we observed small alcohol spots on the inter-phase of the solution film while flowing down over the tubes. These spots gathered at the bottom tray where the outlet solution from the absorber was collected (see Fig. 9). However we did not observe these spots when

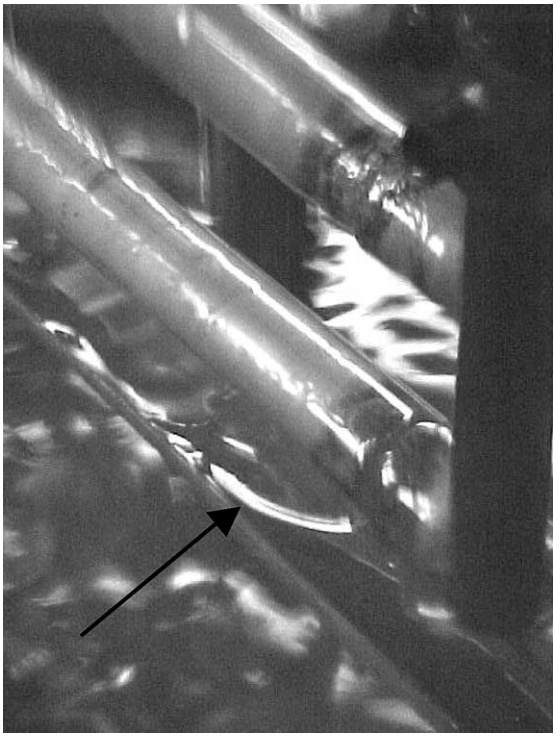

Fig. 9. Detail of the tray at the bottom of the absorber. When no unstable flow was seen, that is film in *S*-region, alcohol was gathered on the surface of the solution after some minutes in the tray. Small spots over the falling film were also observed.

interfacial turbulence was present either in the falling film or in the tray.

The Soret effect has a strong dependence on the solution concentration and temperature. Roughly; the higher the salt concentration the smaller the Soret effect, the lower the temperature the higher the sensibility of the Soret effect to the salt concentration.

According to our plan, in what follows we will use this plane to compare theory and experience. The corresponding tested points without additive (corresponding to those in [12]), are also represented just for comparison purposes, in the same Ma'–Re co-ordinate plot. This is not strictly right since in this case $\partial\sigma/\partial T$ would have a negative sign but it serves to compare

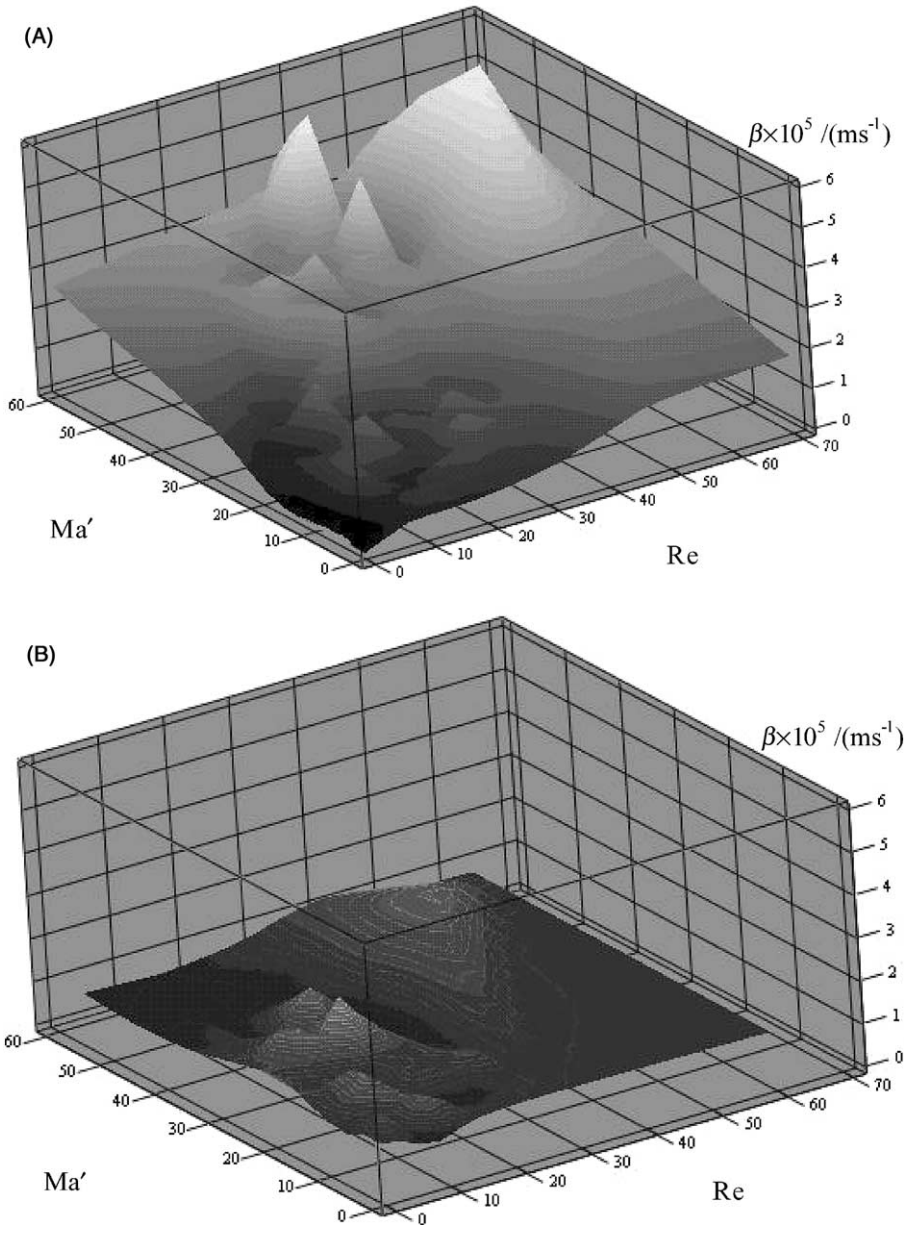

Fig. 10. Surface plot connecting the measured mass transfer coefficients for each run of the multi-factorial test, as a function of the Reynolds number and the modified Marangoni number Ma': (A) with additive and (B) without additive. Notice, for case with additive, the high values for high enough Ma' and $Re > 40$.

values for points working at similar conditions but for the presence of the additive. The points with and without additive have been used to build the surface plots in the figures of the following section.

5.2. Discussion

In Fig. 10 it is shown the surface plot of the mass transfer coefficient. Fig. 8 represents the projection of the points from this plot onto the Re–β plane.

The first time that a small amount of alcohol was added to the vapour phase, the solution concentration and the peripherical flow rate were at its high and low level respectively. The amount of alcohol was around 30 M ppm. It was expected a visual change in the hydrodynamic conditions, according to the literature [10,13]. However, surprisingly no change was appreciated visually. After checking that the plant was operating properly we continued with the tests. In the following tests, as the solution concentration decreased we observed a change in the hydrodynamics. The post-processing of the data showed that something else was going on. As was mentioned in the previous section, assuming that a strong correlation exists between the mass transfer coefficient β and the surface turbulence, the comparison between Figs. 10 and 3, seems to indicate that perhaps a sort of stability window does exist. It must be kept in mind that according to what has been suggested the Soret effect would also influence the surface tension dynamics and therefore would modify the Ma number and hence it might also contribute to explain the decrease in β due to a reduction in Ma when the salt concentration raises.

One point, in favour about the stability window, is that firstly it would explain why we did not see, for the whole absorber, any change in the flow pattern the first time we added the alcohol. Secondly, we realised afterwards, about the existence in any subsequent run, of a curious flow pattern on the first tube—just below the distributor—see Fig. 11. Under each jet below the distributor a very narrow ring was formed and between the impinging jets, on the first tube, a very vibrating thin film of solution was formed. The ring width and its wriggling, although always present, seemed to depend on the absorption rate of the whole the run. The higher the absorption rate the narrower and the more static the ring remained. We suspect that just below the distributor as the local Reynolds number is higher than the medium Reynolds, computed for the whole absorber width because of the jet distribution system, the absorption process in locally unstable for the first tube (even for the lower Γ). In the span-wise direction, according to the 3D theoretical studies, the flow is unstable leading to a very thin film and due to the solution flow coming from the jets a thicker ring is formed at the section of the tube just below that jet.

This latter observation supports the idea that if the tested run has its Ma'–Re co-ordinates in the unstable zone of the window, the experience gives a measured β value higher than the value without additive, pointing out that a surface renewal is ongoing due to a instability.

Fig. 12 shows the contour plot of rq. As before Fig. 7 is the projection of the points from this plot onto the Re–rq plane. The plot shows that rq raises sharply for low Reynolds numbers or—equivalently—low peripherical mass flow rates Γ or high salt concentrations—that is,

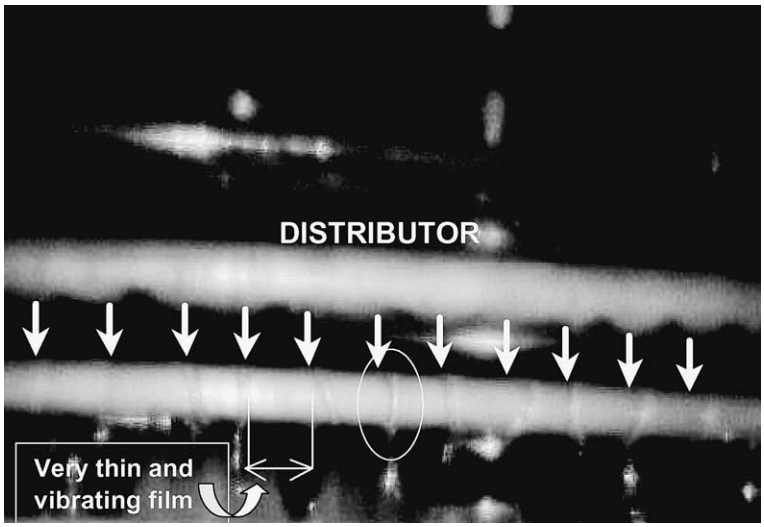

Fig. 11. Detail of the distributor and the first tube (from the top). In all the runs a thick ring of solution was formed just below each falling jet from the distributor. The space between the rings on the first tube was covered by a very vibrating and thin film. The photo is not of a very good quality because this effect was not expected.

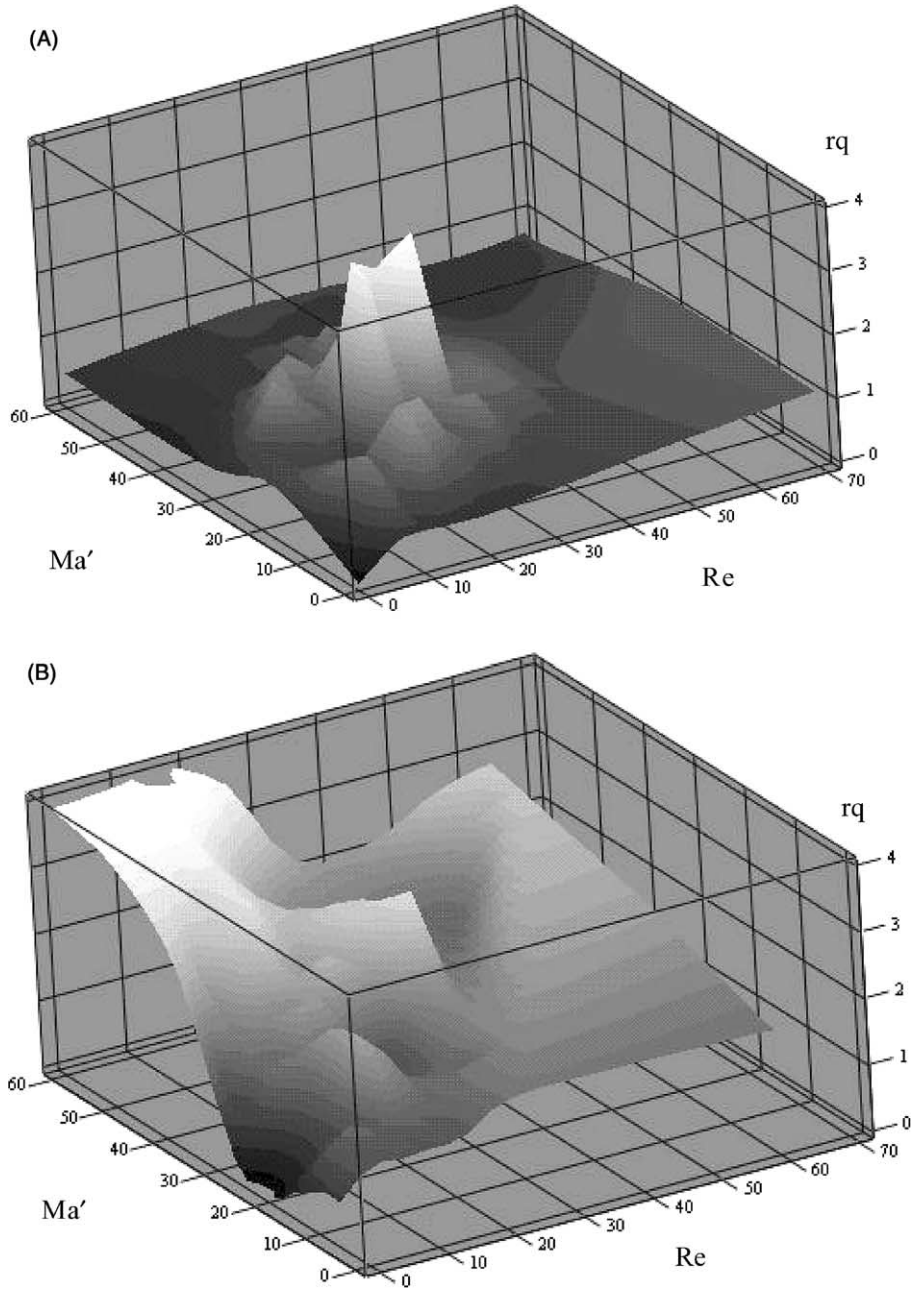

Fig. 12. Surface plot connecting the measured heat ratios (*rq*) for each run of the multi-factorial test as a function of the Reynolds number and the modified Marangoni number *Ma*′: (A) with additive and (B) without additive. Notice that the graphs look like inverse one of the other. Low values of *rq* are of interest. The low *Re* region is very worse for the case with additive since the absorption process seems to stop (be hindered).

within the hypothetical stability window. That means a great amount of sensible cooling because of the increase in the resistance to absorption. Moreover if similar points from the NA and A groups are compared within this zone something can be concluded.

The points from the NA have lower *rq* (less sensible cooling) than the points from A. The first have a thin film thickness because of their low Reynolds. However the second ones, despite the film should have also of the same thickness, have also additive in a stable film and

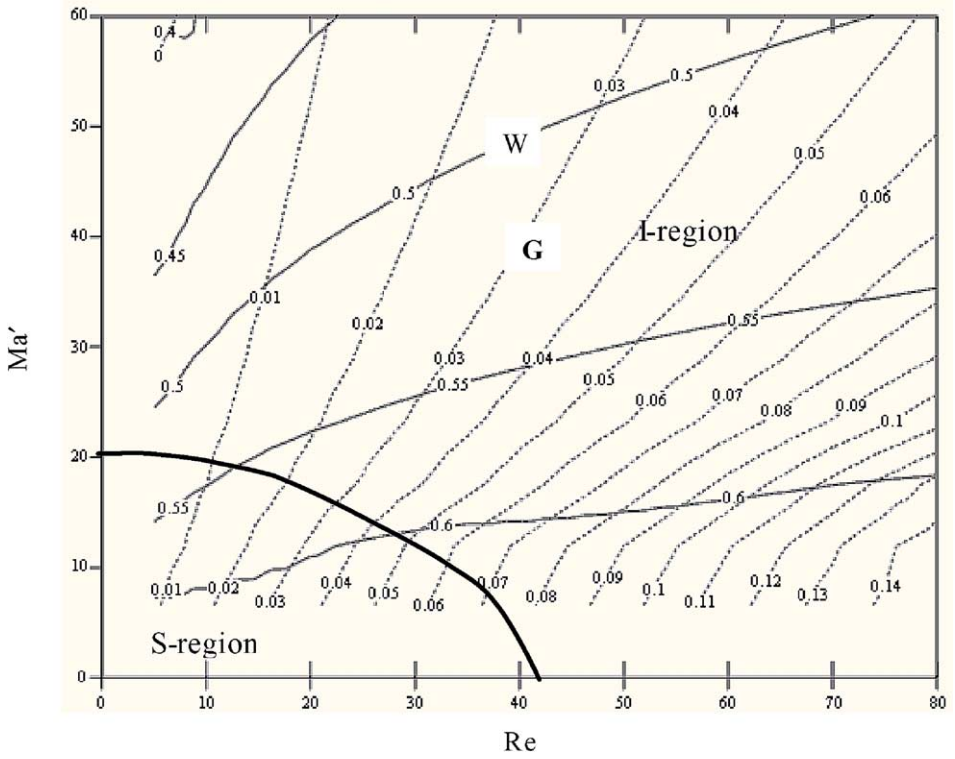

Fig. 13. The graph shows the relationship between the modified Marangoni number Ma' and the Reynolds number (Eqs. (10) and (11)) as a function of more practical variables: like the solution concentration and peripherical mass flow rate Γ ($\mathrm{kg\,m^{-1}\,s^{-1}}$). The line represents the estimated (according to our study) surface Σ_s which divides the plane into the *S*-region and *I*-region. More exactly the graph represents how these regions might be reached by the LiBr solution when properties are calculated at 40 °C and a temperature difference between the inter-phase and the tube surface of $\Delta T = 10$ °C has been used.

this seems to be increasing the resistance to mass transfer very much, thus leading to a much higher *rq*. During the tests no "vibration " on the surface and an increase in the pressure could be observed under these conditions.

However, the tendency is the opposite outside the stability window. The points of NA have an increasing film thickness, which produces a higher resistance to mass transfer and leads to higher *rq*. When the additive was present they were able to produce the instability and outside the stability window the *rq* decreases sharply even below unity.

Finally, in order to relate the points on the Ma'–*Re* plane with operational and/or physical parameters of the absorber, Fig. 13 has been prepared. This figure has been calculated exclusively with the physical properties of the solution at $T = 40$ °C and with a $\Delta T = 10$ °C for the Ma' in Eq. (12). The solid line separates approximately what seems to be the stability window according to our multi-factorial test and Figs. 10 and 12. Therefore it seems, that in the limit of pure hydro-dynamical and capillary-dynamical, the critical values of the *Re* and Ma' numbers (those values where the solid line in Fig. 13 crosses the *Re* and *Ma* axis respectively) are around 40 and 20 respectively.

One very interesting practical issue is that if the peripherical mass flow rate Γ is kept constant (for instance at 0.04 $\mathrm{kg\,m^{-1}\,s^{-1}}$) but the LiBr concentration is increased, the working conditions of the absorber will get closer or even into the stability zone of the film (see Fig. 13). Under this state the film will suffer a high sensible cooling and very little water vapour will be absorbed due to the transfer resistance produced by the additive at the inter-phase. In short; the absorption process stops. A way to avoid such situation could be increasing Γ or/and the solution re-circulation flow ratio onto the absorber to reduce the inlet concentration or in one word, rise the Reynolds number.

6. Conclusions

The outcome of this work is to present the results of heat and mass transfer during absorption with a surfactant in a methodological way, following the procedure used previously in [12]. The mathematical

treatment in this case is very complex due to the presence of instabilities. This is the reason why the review in Section 3 of the specialised literature about the subject has been preferred mainly about falling films.

The results from the multi-factorial experiences have shown the interaction between the different variables chosen in the study. Taking this into account and after the comparison of the experimental and theoretical works on stability of films, the possibility of existence of a *stability window* for the film during the absorption was concluded. The instability is controlled by the Reynolds and Marangoni numbers. Both numbers are very sensitive to the solution concentration, mainly because of the change of its viscosity. In particular, the Marangoni number depends linearly on the $\partial\sigma/\partial T$ and from the previous results without additive [12], we think that the Soret effect could be involved in the dynamic behaviour of the surface tension and therefore could be influencing—along with the amount of additive—the value of this derivative. The presented results are coherent with this hypothesis.

Contrarily to the a wide spread opinion that the mass transfer in LiBr absorbers is the limiting process, we think that under certain conditions this is not the case. A non-desirable situation is also possible; if the mass transfer is good enough, the heat released during absorption may be higher than the one gone to the cooling water and therefore it is needed an extra heat-only (without absorbing this time) removing capacity. In other words, the mass transfer is not acting as the "bottle neck" when additive is present and the instability-controlling parameters (*Ma* and *Re*) are chosen properly so as to destabilise enough the film. In fact, in our tests we actually did not expect this situation and unfortunately we were constrained by the set-up design to $Re < 70$. However our feeling is that there is still room for rising the Reynolds number in order to raise the mass transfer coefficient much more than in the present study.

This study gives insight into the horizontal tube absorber behaviour and indicates how both transfer processes could be controlled. The *Re* and *Ma* are very sensitive to the inlet salt concentration as Fig. 13 shows and also to the inlet temperature. Practical indirect variables to control the transfer process could be: the peripherical mass flow rate Γ and the re-circulation mass flow at the absorber, in order to control de inlet concentration and the operating Reynolds.

From the experimental results it seems that in order to achieve a reduction in size of the absorber section a combination of an horizontal tube absorber working at as high mass transfer rates as possible (by searching high instabilities in the Ma'–Re plane) and a controlled post-cooling of the outlet solution just to achieve a global $rq = 1$ of the whole process. This last cooling should be done without absorption. We think this could be an interesting possibility and the integration of such a system into a complete absorption cooling machine will be a work for the future.

This proposal should not be confused with what is known as adiabatic absorption (see for instance Ryan [27]). In opposition to [27], where after a previous subcooling of the solution, the absorption takes place without an external heat transfer, here we do need a simultaneous cooling during absorption so as to achieve a high enough *Ma* number (obviously, with simultaneously a high enough *Re*), which would lead the falling film into the unstable region therefore promoting the mass transfer.

Finally, as a work which is still to be done we can point out that from the fact that there is the change in the behaviour for concrete values of the Reynolds number (as we have shown at 40 in the case with additive and at 30 without additive—see for this last case Soto Francés and Pinazo Ojer [12] or Nosoko et al. [28]) and from the fact that the maximum perturbing wavelength that can be imposed to the film thickness is one half of the tube perimeter, we suspect that some interesting actual dynamical properties can be inferred from the comparison of theoretical studies and experimental results (like actual viscosity relaxation phenomena during absorption due to the high frequency surface vibrations. See Dandapat and Mukhopadhayay [29] for the dependence of the critical Reynolds on such phenomena). But more theoretical research is needed mainly for falling films over round tubes.

Besides, despite the existence of some theories about surfactants, the dynamical action of the additive at the inter-phase (see [24,25]) remains not well understood to our knowledge and the implication—or not—of the Soret effect in its action should also be clarified.

Acknowledgements

We would like to thank the DGESIC (Dirección General de Enseñanza Superior e Investigación Científica) of the Spanish Goverment, for its financial support under the research project PB97-0336-C02 and the Universidad Politécnica de Valencia, by its support with the project no. 24 of the Plan de Innovación Tecnolgica y Artística. We would like to thank also the comments of the referees in order to expose more clearly this complex subject.

References

[1] R. Tozer, B. Agnew, Optimisation of ideal absorption cycles with external irreversibilities, in: Proceedings of the International Sorption Heat Pump Conference, Munich, 1999, pp. 453–457.

[2] F. Ziegler, Discussion of optimised design of endo-reversible heat transformation cycles, in: Proceedings of the International Sorption Heat Pump Conference, Munich, 1999, pp. 459–464.
[3] V.M. Soto Francés, J.M. Pinazo Ojer, Experimental study about heat and mass transfer during absoprtion of water by an aqueous lithium bromide solution, in: Proceedings of the ASME-ZSITS Int. Thermal Science Seminar, Bled, Slovenia, 2000, pp. 535–541.
[4] J.R. Pearson, On convection cells induced by surface tension, J. Fluids Mech. 4 (1958) 489–500.
[5] T. Kashiwagi, Y. Kurosaki, H. Shishido, Enhancement of vapour absorption into a solution using the Marangoni effect (1st report, Mechanism for the inducement of the Marangoni convection and effects of steam absorption enhancement by the addition of higher alcohol), Trans. Jpn. Soc. Mech. Eng. Serv. B 51 (463) (1985) 1002–1009.
[6] H. Daiguji, E. Hihara, Y. Saito, Mechanism of absorption enhacement by surfactant, Int. J. Heat Mass Transfer 40 (8) (1997) 1743–1752.
[7] E. Hihara, T. Saito, Effect of surfactant on falling film absorption, Int. J. Refrig. 16 (15) (1993) 339–346.
[8] F. Ziegler, G. Grossman, Review paper: Heat-transfer enhancement by additives, Int. J. Refrig. 19 (5) (1996) 301–309.
[9] H. Pérez-Blanco, W. Del Cul, J. Braunstein, R.H. Reiner, Experimental study of the effect of additives on mass transfer to an aqueous solution of lithium bromide, in: ASME National Heat Transfer Conference Minneapolis, July 28–31, 1991.
[10] W.A. Miller, The synergism between heat and mass transfer additive and advanced surfaces in aqueous LiBr horizontal tube absorbers, in: ISHPC '99 Proceedings of the International Sorption Heat Pump Conference, Munich, Germany, 1999, pp. 307–321.
[11] I. Greiter, A. Wagner, V. Weiss, G. Alefeld, Experimental investigation of heat and mass transfer in a horizontal-tube falling-film absorber with aqueous solutions, in: AES-vol.31 Int. Absorption Heat Pump Conference, 1993, pp. 225–232.
[12] V.M. Soto Francés, J.M. Pinazo Ojer, Validation of a model for the absorption process of H_2O(vap) by a LiBr(aq) over an horizontal tube bundle using a multifactorial analysis, Int. J. Heat Mass Transfer 46 (17) (2003) 3299–3312.
[13] I.-S. Kyung, K.E. Herold, Performance of horizontal smooth tube absorber with and without 2-ethyl-hexanol, J. Heat Transfer 124 (2002) 177–183.
[14] V.M. Soto Francés, Transferencia de calor y masa en absorbedores de tubos horizontales que trabajan con la mezcla LiBr–H_2O, Tesis doctoral, Valencia, España, 2000.
[15] H. Lars, Bestimmung von Wärmeübergangskoeffizienten wssriger LiBr-Lösung mit und ohne Zusatz oberflchenaktiver Substanzen auf einem Absorberwärmetauscher, Diplomarbeit Institut E19 Physik_department der Technichen Univertät München, 1994.
[16] Engineering Statistics Handbook. Available from <http://www.itl.nist.gov/div898/handbook/pri/section5/pri597.htm>.
[17] I. Fujita, E. Hihara, Surface tension-driven instability of thin liquid film of LiBr aqueous solution absorbing water vapour, in: ISHPC'99 Proceedings of the International Sorption Heat Pump Conference, Munich, Germany, March 24–26, 1999, pp. 367–373.
[18] S.W. Joo, S.H. Davis, S.G. Bankoff, Long-wave instabilities of heated falling films: two-dimensional theory of uniform layers, J. Fluid Mech. 230 (1991) 117–146.
[19] R.Kh. Zeytounian, The Bérnard–Marangoni thermocapillary-instability problem, Physics-Uspekhi Fizicheskikh Nauk, Russ. Acad. Sci. 41 (3) (1998) 241–267 (in English).
[20] P.L. Kapitza, S.P. Kapitza, Collected Works, Pergamon, 1965, pp. 690–709.
[21] S.W. Joo, S.H. Davis, Instabilities of three-dimensional viscous falling films, J. Fluid Mech. 242 (1992) 529–547.
[22] S.W. Joo, S.H. Davis, S.G. Bankoff, A mechanism for rivulet formation in heated falling films, J. Fluid Mech. 31 (1996) 279–298.
[23] C. Kren, H.M. Hellmann, F. Ziegler, Dynamic surface tension of lithium bromide-solutions with higher alcohols as heat-transfer additives, in: Proceedings of the International Sorption Heat Pump Conference, ISHP Munich, Germany, 1999, pp. 375–380.
[24] S.M. Bennett, The Effect of Surfactants on Steam Absorption onto Lithium Bromide Solution, M.S. Thesis, Penn State University, 1995.
[25] K. Satheesh, K.E. Herold, Theory of Heat/Mass transfer additives in absorption chillers, HVAC&R Res. 6 (4) (2000) 369–380.
[26] J. Colombani, J. Bert, J. Dupuy-Philon, Thermal diffusion in (LiCl, RH_2O), J. Chem. Phys. 110 (17) (1999) 8622–8627.
[27] A.W. Ryan, Water absorption in an adiabatic spray of aqueous lithium bromide solution, in: Proceedings of the International Absorption Conference AES-vol31, 1993, pp. 155–162.
[28] T. Nosoko, A. Miyara, T. Nagata, Characteristics of falling film on completely wetted horizontal tubes and the associated gas absorption, Int. J. Heat Mass Transfer 45 (2002) 2729–2738.
[29] B.S. Dandapat, A. Mukhopadhayay, Waves on a film of power-law fluid flowing down an inclined plane at moderate Reynolds number, Fluid Dyn. Res. 29 (2001) 199–220.